Relativistic hydrodynamics of partially stopped baryonic matter

J. Bolz,[1,*] U. Ornik,[1,2,†] and R. M. Weiner[1,‡]
[1]*Physics Department, University of Marburg, Marburg, Federal Republic of Germany*
[2]*Theoretical Divison, Los Alamos National Laboratory, Los Alamos, New Mexico 87545*
(Received 18 May 1992)

Relativistic hydrodynamics including final-state interactions is used for a detailed description of the experimental data on particle spectra of sulphur-sulphur collisions at 200A GeV from the $NA35$ Collaboration. Under the assumption of thermalization of the entire detected baryonic matter it is found that a consistent reproduction of both pion and proton spectra requires strong stopping as an initial condition for the expanding fireball. The results from these calculations are then used to extract a transverse radius which includes also contributions from the decay of unstable particle resonances. Its value is found to be rapidity dependent within the range of 3–4 fm, which agrees with experimental results from Bose-Einstein correlations. In addition, the analysis of the strange particle distribution indicates chemical equilibrium for K^0 and Λ particles.

PACS number(s): 25.75.+r, 12.40.Ee, 13.85.Ni, 14.20.−c

I. INTRODUCTION

Statistical and hydrodynamical concepts have been successfully used for the description of multiparticle production in strong interactions. Within the hydrodynamical picture of a relativistic heavy-ion reaction one can divide the evolution of the system into three stages: First there is a compression and thermalization of nuclear matter, then this highly excited fireball begins to expand according to the laws of relativistic hydrodynamics, and finally the system decouples and particles are emitted. The description of the second and the third stage can be given in a more or less straightforward manner, whereas there are severe problems in the treatment of the first stage due to the lack of knowledge about the soft-QCD interactions, the very short time scale and thus the restricted applicability of thermodynamical concepts. This first step in the evolution of the system is usually described by initial conditions. One of the main tasks of research in this field is to investigate the details of this first stage and the present paper is an attempt in this direction. In particular, we look at some new aspects of the application of hydrodynamics to heavy ion collisions by including the consideration of baryons, the spectra of which have been measured very recently. It turns out that the information about baryons modifies substantially our knowledge about the initial system and especially about the amount of stopping power. Using an exact solution of three-dimensional hydrodynamics we are also able to estimate the transverse radius of the nuclear fireball and to investigate the production of strange particles which is sensitive to the existence of the quark-gluon-plasma (QGP) phase. All calculations presented here include resonance production and the influence of the subsequent decay on the particle system.

II. INITIAL CONDITIONS

There are two types of initial conditions in the hydrodynamics of high energy collisions: Landau-type initial conditions and Bjorken-type initial conditions. In the original formulation of Landau [1], the system is assumed to be completely stopped and the entire energy is deposited in an initial volume, the longitudinal size of which is Lorentz contracted by the factor

$$\gamma = E/m \ ,$$

where E is the projectile energy in the equal-velocity frame and m its mass. This energy is thermalized and becomes available for particle production. Subsequently, after the discovery of the leading-particle effect, the inelasticity concept was introduced in the Landau model by postulating that only a fraction

$$K = M/\sqrt{s}$$

called "inelasticity" is locally thermalized and contributes to particle production [2,3]. Here M is the invariant mass of the system. Furthermore, with the introduction of an effective Lorentz contraction $\gamma' = K\gamma$ [2–4] and the determination of the longitudinal extension of the source in agreement with the uncertainty relation many of the experimental data in hadron-hadron as well as heavy ion collisions in the available energy range (2 GeV $< \sqrt{s} <$ 1800 GeV)[1] could be explained (see, e.g., Refs. [5–7]).

*Electronic address:BOLZ-J@DMRHRZ11
†Electronic address: ORNIK@DDAGSI5
‡Electronic address: WEINER@DMRHRZ11

[1]Here $\sqrt{s}$ refers to the nucleon-nucleon system.

In the case of Bjorken-type initial conditions the system is emitted from a pointlike source, rapidity-boost invariant and thermalized after a proper time of the order of 1 fm [8]. The experimental fact known for many years that the rapidity distribution of secondaries is not plateaulike strongly suggests that this condition as such cannot be maintained.

However, new experimental data by the NA35 Collaboration on sulphur-sulphur collisions at 200 GeV/nucleon indicate that (a) also has to be modified and this is one of the main results of the present investigation. Both types of initial conditions refer to reactions in which no baryons are stopped in the central region and therefore are clearly separated in phase space from the central fireball. Such a behavior has been observed in high energy nucleon-nucleon reactions (leading particle effect) and is also expected to occur in heavy ion collisions at energies much higher than presently accessible. The $S+S$ data of the NA35 Collaboration at 200 GeV/nucleon however suggests that baryons are present in the central region and their final (observed) distribution is more or less uniform with indictions of two slight peaks at rapidities ± 2 (cf. Figs. 2 and 5). As will be explicitly proved in the following this however does not imply that the *initial* baryon distribution is uniform as would be expected in the case of boost invariance (cf. below).

As long as no baryons were present the Landau initial conditions were fixed by giving (i) the longitudinal initial size Δ of the system (Lorentz contracted) and (ii) the energy U_{Landau} deposited in this region. A time scale t_a for the initial conditions is given by the time it takes for two nuclei at the speed of light to penetrate each other. This scale is of the order of 1 fm/c and it serves as a causal limit for the longitudinal extension of the whole system. In our new model we additionally impose an initial rapidity field $y(z)$ on the fluid. Its modulus is supposed to be a function only of the longitudinal coordinate z with its shape constrained by two boundary values: The rapidity should vanish at $z=0$ and asymptotically reach its maximum value $|y_{\text{c.m.}}|$ at $z=\pm t_a$ ($y_{\text{c.m.}}$ being the center-of-mass rapidity). Thus the two parameters of the original Landau approach have to be supplemented by giving the function $y(z)$ which we parametrize by the free parameter a_y as

$$y(z)=y_{\text{c.m.}}\tanh(a_y z) \tag{1}$$

and the initial baryon-rapidity distribution, for which we write

$$\frac{db}{dy}=C_y(e^{-(y-y_m)^2/2\sigma^2}+e^{-(y+y_m)^2/2\sigma^2}) \tag{2}$$

and which depends on two parameters y_m and the width σ. C_y is a normalization constant the value of which can be determined from the requirement that (2) integrated over the whole accessible rapidity interval is equal to the total baryon number of the system. A spatial baryon distribution is then easily derived from Eqs. (1) and (2):

$$B_0(z)=\frac{1}{\pi R^2}\frac{db}{dy}\frac{dy}{dz}\ , \tag{3}$$

where R is the radius of the cylindrical fireball. Thus the initial volume in which the baryons are located is somewhat bigger than the Landau volume. Note that B_0 is the baryon density in the equal-velocity frame, which is the 0 component of the baryon-four current

$$B^\mu=bu^\mu\ .$$

Here b is the baryon-density in the rest frame of a fluid cell with four-velocity u^μ.

Because only a fraction K_{part} of all participant nucleons is really detected in experiment, the total c.m. energy and the total baryon number of the system should be multiplied by a factor K_{part}, which is about 85% in the NA35 experiment [9].

The total energy $E_{\text{tot}}=K_{\text{part}}\sqrt{s}$ of the system is composed of three parts:

$$E_{\text{tot}}=U_{\text{Landau}}+U_{\text{out}}+E_{\text{kin}}\ , \tag{4}$$

where E_{kin} is the kinetic energy of the fluid and U_{Landau} and U_{out} are the thermal energies inside and outside the Landau volume, respectively. Their densities are given as follows:

$$\begin{aligned}
&\epsilon_{\text{kin}}(z)=\epsilon(z)(1+c^2)u_1^2\ ,\\
&\epsilon(z)=\begin{cases}\epsilon_{\text{Landau}}(z) & \text{if } |z|<\Delta/2\ ,\\ \epsilon_{\text{out}}(z) & \text{if } |z|\geq\Delta/2\ ,\end{cases}\\
&\epsilon_{\text{Landau}}(z)=\text{const}\ ,\\
&\epsilon_{\text{out}}(z)=b(z)m_N(1+\kappa\{\cosh[y_{\text{c.m.}}-y(z)]-1\})\ ,
\end{aligned} \tag{5}$$

where m_N denotes the nucleon mass and $c^2=p/\epsilon$ is given by the equation-of-state (cf. next section). Instead of ϵ_{Landau} we take as a parameter the fraction $K_L=U_{\text{Landau}}/E_{\text{tot}}$. The ansatz for ϵ_{out} is motivated by the assumption that for a single nucleon the amount of thermal energy (in its rest system after the collision) is proportional to the loss of kinetic energy in the longitudinal direction which is $m_N\{\cosh[y_{\text{c.m.}}-y(z)]-1\}$. The proportionality constant κ can be determined by the demand that integration of the density of kinetic and thermal energy over the whole system yields the value E_{tot}.

To summarize, there are five parameters in this model which fix the initial conditions of the fireball: (i) The length Δ of the Landau volume; (ii) the fraction K_L of thermal energy inside the Landau volume which corresponds to ϵ_{Landau}; (iii) the absolute value of rapidity at $z=\pm\Delta/2$, denoted by y_Δ, which determines the slope parameter a_y of Eq. (1); and (iv) the parameters y_m and σ of the double-Gaussian initial rapidity distribution of the baryonic charge.

Table I shows the values of all these quantities. In particular, for the length parameter Δ we obtained a value of 0.7 fm. A model with compression shocks as that proposed by Belenkij and Milekhin [10] suggests a smaller value of 0.45 fm. Nearly the same number can be obtained by the mechanism described in Ref. [7] which explicitly uses the uncertainty relation to estimate a lower bound for the longitudinal localization of the system.

TABLE I. Initial fireball quantities describing the experimental $S+S$ data.

Given by experiment	
Total available energy E_{tot}	528.1 GeV
Total baryon number	54.4
c.m. rapidity $y_{\text{c.m.}}$	3.028
Radial extension R of Landau volume	3.81 fm
Free parameters of the model	
Fraction K_L of thermal energy in Landau volume	43.5%
Longitudinal extension Δ of Landau volume	0.7 fm
Rapidity y_Δ at edge of Landau volume	0.9
Parameter y_m of initial baryon y distribution	0.82
Parameter σ of initial baryon y distribution	0.4
Derived quantities	
Parameter a_y in Eq. (1)	0.876 fm^{-1}
Parameter κ in Eq. (6)	1.718
Fraction of baryonic charge inside Landau volume	49.8%
Lifetime of the system	5.3 fm/c
Thermal energy U_{Landau} in Landau volume	22918 GeV
Thermal energy U_{out} outside Landau volume	66.7 GeV
Total kinetic energy E_{kin}	231.6 GeV
Energy-density ϵ_{Landau} in Landau volume	7.2 GeV/fm^3
Temperature in Landau volume	228 MeV

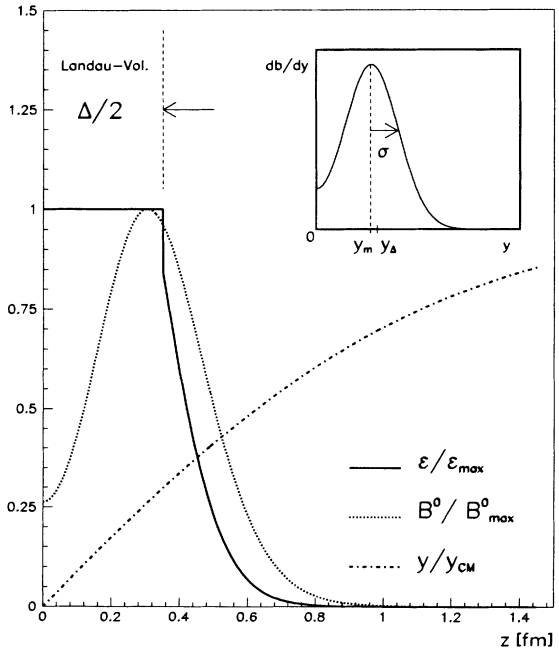

FIG. 1. Initial distributions of energy and baryon density, as well as the rapidity, normalized to their maximum values and plotted against the longitudinal coordinate z. In the upper right corner we give also the rapidity distribution of the baryonic-charge. The parameters are chosen according to Table I.

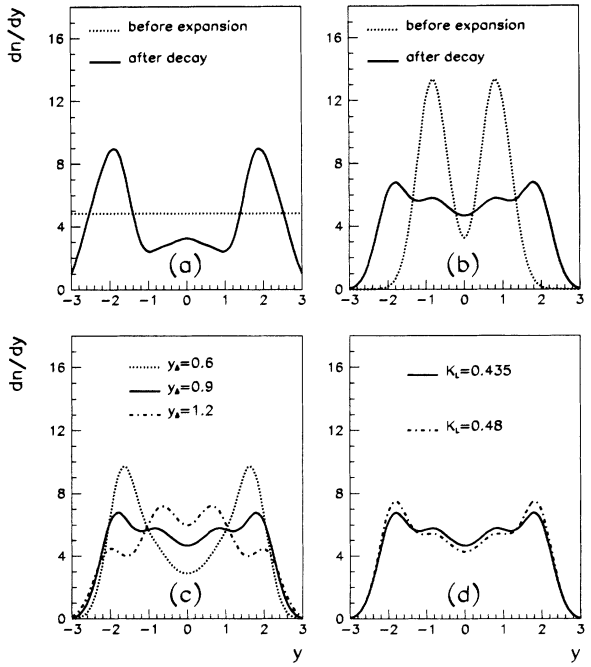

FIG. 2. (a) and (b) illustrate the effect of hydrodynamical expansion and final-state interaction on the proton-rapidity distributions. Dashed are the initial distributions and solid those after freeze-out and decay of particle-resonances. For (b) we chose the "correct" initial parameters (cf. Table I). The plots (c) and (d) demonstrate different choices of initial parameters. The solid curves are identical with that of (b) and for all other curves only the quoted parameters differ from those in (b).

Compared to this the modified Landau model without compression shocks gives a value 1.5 fm ($=2R/K\gamma$). So our value is between these two limiting cases but is closer to the lower bound given simultaneously by the shock-wave and the uncertainty-relation approach.

In Fig. 1 we give the initial spatial distributions of energy and baryon density, as well as the rapidity field, which lead to satisfactory spectra of pions and protons (see the section "results"). We have tried different variants of parameters and found among other things that an initial uniform rapidity distribution of the baryons does not lead to the observed distribution. This and other attempts are illustrated in Fig. 2. As can also be seen there the "correct" initial baryon distribution is sharply peaked at comparatively low rapidity values giving rise to strong stopping. This means that the majority of baryons is accelerated to high rapidities by the internal hydrodynamical pressure. The latter is growing with the initial concentration of baryonic matter and can thus be controlled by the parameter y_Δ, because according to Eq. (3) $B_0(z)$ is proportional to the slope of $y(z)$. A modification of the length Δ at fixed K_L only slightly influences the final proton-rapidity distribution and is thus not shown in Fig. 2, whereas the increase of K_L, the other parameters being kept fixed, leads to a sharpening of the rapidity peaks.

III. THE HYDRODYNAMICAL MODEL

A. Hydrodynamical expansion

After specifying the initial conditions the nuclear matter is treated as an ideal relativistic fluid obeying the laws of hydrodynamics which are written in a brief form as follows:

$$\partial_\mu T^{\mu\nu}=0\ ,\quad \partial_\mu B^\mu=0\ ,$$
$$T^{\mu\nu}=(\epsilon+P)u^\mu u^\nu-Pg^{\mu\nu}\ ,\quad B^\mu=bu^\mu\ . \tag{6}$$

The equation of state (EOS) is written

$$P=c^2(\epsilon,b)\epsilon\ . \tag{7}$$

This coupled system of partial differential equations is solved numerically in 3+1 dimensions by the program HYLANDER.[2] For the EOS we chose a parametrization of results from lattice QCD with a first order phase transition from hadronic matter to quark-gluon plasma. Unfortunately the presence of baryons (fermions) is not yet introduced in the EOS. It is well known that this is a yet unsolved problem in statistical QCD. Nevertheless the present approach which considers explicitly baryons in the equations of hydrodynamical expansion is a step forward towards the solution of this complex problem and we do not expect drastic changes from the introduction of baryons in the EOS. Although lattice QCD does not yet permit the introduction of baryons in the EOS, there are phenomenological models which allow this (Ref. [11], cf. also the note at the end of the paper). This problem is under investigation.

[2]Hydrodynamical Landau expansion routine.

The choice of the EOS mentioned above is due to our previous findings for the reaction $O^{16}+Au^{197}$ at 200 GeV/nucleon [5], that other EOS which do not include a QCD-phase transition lead to unacceptable results for the rapidity distribution of secondaries. This observation has been recently supported by the hydrodynamical investigations of Ishii and Muroya [11].[3] In $S+S$ at the same energy, which is the subject of the present investigation, the initial energy density is higher and therefore the use of an EOS with a QGP is even more compelling.

B. Freeze-out and final-state interactions

In the hydrodynamical model particles are supposed to decouple from the fireball if their mean free path exceeds the dimension of the system. In the picture of an expanding fluid the former is connected to the local temperature of a given fluid cell. Thus as a criterion for the so-called "freeze-out" one chooses a critical temperature T_f of the order of the pion-mass at which particles are emitted from the fireball.

Collecting all space-time points of temperature T_f to a hypersurface in Minkowski space, one can give the momentum distribution of a particle of four-momentum p^μ in terms of the generalized Cooper-Frye-Schonberg formula (see Ref. [12])

$$E\frac{dn}{d^3p}=\frac{g}{(2\pi)^3}\int_\Sigma \frac{p^\mu d\sigma_\mu}{\exp[(p^\mu u_\mu-b_i\mu_B-s_i\mu_S)/T_f)]\pm 1}\ , \tag{8}$$

where g denotes the degeneracy factor of the particle and the sign in the denominator of the integrand depends on whether one deals with bosons or fermions. Σ is the freeze-out hypersurface, u^μ is the four-velocity of the element $d\sigma_\mu$ and μ_B and μ_S are the baryon and strangeness chemical potential, respectively. These potentials have to be introduced, because the assumption of chemical equilibrium requires zero strangeness and (in general) nonzero baryon density at each freeze-out point (the baryon number couples to strangeness via hyperons like Λ and Σ). In detail one has to solve the following system of equations for each surface point of given baryon density b in its rest frame:

$$\sum_i b_i n_i(\mu_B,\mu_S)=b\ ,$$
$$\sum_i s_i n_i(\mu_B,\mu_S)=s=0\ , \tag{9}$$

where the index i enumerates all resonances and their antiparticles. b_i, s_i, and $n_i(\mu_B,\mu_S)$ denote the corresponding baryon number, strangeness, and number density[4] of the ith resonance, respectively. In Table II we give a list

[3]This is even more interesting as in [11] different initial conditions were used.

[4]This is given by a Bose or Fermi distribution integrated over the whole momentum space with mass, chemical potential, and degeneracy factor of the particle properly taken into account.

TABLE II. Particle resonances included in this calculation.

Name	m/MeV	Spin	B	S	I	Decays
			Mesons			
π	139	0	0	0	1	stable
K^+	494	1/2	0	1	1/2	stable
K_L^0	494	1/2	0	1	1/2	stable
K_S^0						2π
η	548	0	0	0	0	3π (56%), 2γ (39%), $\pi^+\pi^-\gamma$ (5%)
ρ	770	1	0	0	1	2π
ω	783	1	0	0	0	3π (90%), $\pi^0\gamma$ (8.5%), $\pi^+\pi^-$ (1.5%)
K^{*+}	892	1/2	0	1	1/2	$K\pi$
K^{*0}	892	1/2	0	1	1/2	$K\pi$
η'	958	0	0	0	0	$2\pi\eta$ (65%), $\rho^0\gamma$ (30%)
			Baryons			
N	938	1/2	1	0	1/2	stable
Λ	1115	1/2	1	−1	0	$N\pi$
Σ	1119	1/2	1	−1	1	$\Sigma^0\to\Lambda\gamma$, $\Sigma^\pm\to N\pi$
Δ	1232	3/2	1	0	3/2	$N\pi$
Ξ	1321	1/2	1	−2	1/2	$\Lambda\pi$
Σ^*	1385	1/2	1	−1	1	$\Lambda\gamma$ (88%), $N\pi$ (12%)

of all particle resonances included in the calculation. For the $S+S$ fireball we obtained on the average a baryon potential of about 310 MeV and a strangeness potential of about 50 MeV. The resulting chemical composition of the source at freeze-out is depicted in Fig. 3. It can be seen there that the pions contribute only about 50% to all directly produced particles. In the following we will refer to particles which do not originate from resonance decay as *direct*. Additional contributions are mainly kaons and baryons (each around 15%). The latter are about 50% nucleons.

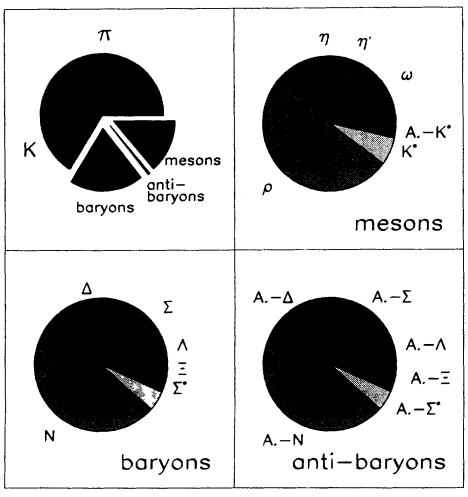

FIG. 3. Chemical composition of frozen-out particles. In the upper left quarter we give a general composition. The subcompositions of the three offset sectors "mesons," "baryons," and "antibaryons" are shown in the remaining parts.

We then calculate the distribution of all stable particles after the decay of resonances. We consider for simplicity only two and three particle decays of resonances. We also took into account the widths of those resonances wherever they exceeded 100 MeV by following the strategy proposed by Sollfrank, Koch, and Heinz in Ref. [13].

The quoted method consists in introducing an additional integration of the Cooper Frye distribution [Eq. (8)] over the mass of the resonance weighted by a Breit-Wigner distribution, where the parametrization of the width Γ of the resonance is derived from a phenomenological potential ansatz for resonance formation(cf. Ref. [14]):

$$\Gamma=\gamma p_0\frac{(p_0r_0)^2}{1+(p_0r_0)^2}\ .$$

r_0 is the range of the scattering potential, Γ the reduced width, and p_0 is the momentum of one of the decay particles in the rest frame of the resonance.

C. Transverse radius

We calculated a transverse radius of the fireball in the same manner as already proposed in Ref. [15] and (in parts) in Refs. [16,17]. This method consists in calculating the space-time distribution of produced hadrons (mostly pions), which are assumed to be created on a hypersurface Σ in Minkowski space and their momentum distribution described by Eq. (8). For the transverse radius $R_\perp$ we then write

$$R_\perp=\frac{\int_\Sigma R\dfrac{p^\mu d\sigma_\mu}{\exp[(p^\mu u_\mu-\mu)/T]\pm1}}{\int_\Sigma\dfrac{p^\mu d\sigma_\mu}{\exp[(p^\mu u_\mu-\mu)/T]+-1}}\ , \tag{10}$$

where u^μ, T, and μ denote four-velocity, temperature, and chemical potential on the hypersurface Σ, respectively. The radius for direct pions ($R_\perp^\pi$) can be calculated directly from Eq. (10), whereas the radii for pions from decay also include the radial distance which unstable particle resonances[5] can travel during their lifetime. Denoting the contribution from the resonance j by $R_\perp^j$ and introducing weight factors w_j for all the contributions one can write

$$R_\perp = w_\pi R_\perp^\pi + \sum_j w_j R_\perp^j \ , \tag{11}$$

To investigate in detail the rapidity dependence of the transverse radius, we remove the dependence on the transverse momentum and the azimuthal angle of momentum by taking the average. Thus we can take for the w_j the relative contribution of the "source" j to the total y distribution of pions. The radius for pions from the decay of the resonance j can be written as

$$\langle R_\perp^j \rangle = \langle \tilde{R}_\perp^j \rangle + \frac{\langle p_{\perp,j} \rangle \tau_j}{m_j} \ , \tag{12}$$

where $\langle p_{\perp,j} \rangle$ and τ_j denote the mean transverse momentum and the lifetime of the resonance j, respectively, and $\langle \tilde{R}_\perp^j \rangle$ is evaluated from Eq. (10) for a particle of mass m_j.

IV. RESULTS

A. Transverse momentum

Our results for the transverse-momentum distributions of negatively charged particles and protons are shown in Fig. 4. Concerning negatives (which are mostly pions) we are able to describe the data both in the central rapidity region ($0 \le y \le 1$) and in the fragmentation region ($1 \le y \le 2.2$). This fact again underlines the nonstationarity in rapidity for heavy-ion-collisions at these energies.

As can also be seen in Fig. 4, resonance decay becomes very important for the transverse-momentum spectrum at low $p_\perp$. There baryonic resonances provide by far their greatest contribution whereas this effect is not so strongly present for the mesonic resonances. A reason for this can be found in the kinematics of decay: A particle which decays into a pion and another particle of much bigger mass gives most of its momentum to the heavier particle. This is the case for baryonic resonances and thus one can easily understand this effect which is discussed in more detail in Refs. [6,13]. The $p_\perp$ distribution of protons is also quite well reproduced by our model.

A few remarks should be made about the experimental data. The proton spectra were gained in a first approximation by subtracting the number of negatively charged particles from the positively charged ones. This can be done because the sulphur nuclei are isospin scalars so that there should be an equal number of π^+ and π^-. Necessary corrections were applied first to account for the nonvanishing strangeness induced by hyperon production which favors the production of K^+ with respect to K^-. The information how to correct the data was taken from a FRITIOF Monte Carlo simulation. As a second important correction, all protons from the decay of Λ particles were subtracted. For this reason we did the same with our results and this distribution is shown in Fig. 4. One must not forget that these corrections of experimental data involve errors because,e.g., the usage of Monte Carlo routines assumes the validity of certain models that need not be consistent with our approach. The apparent slight overestimate of low $p_\perp$ baryons (cf. Fig. 4) is a one standard deviation effect and thus not significant from our point of view.

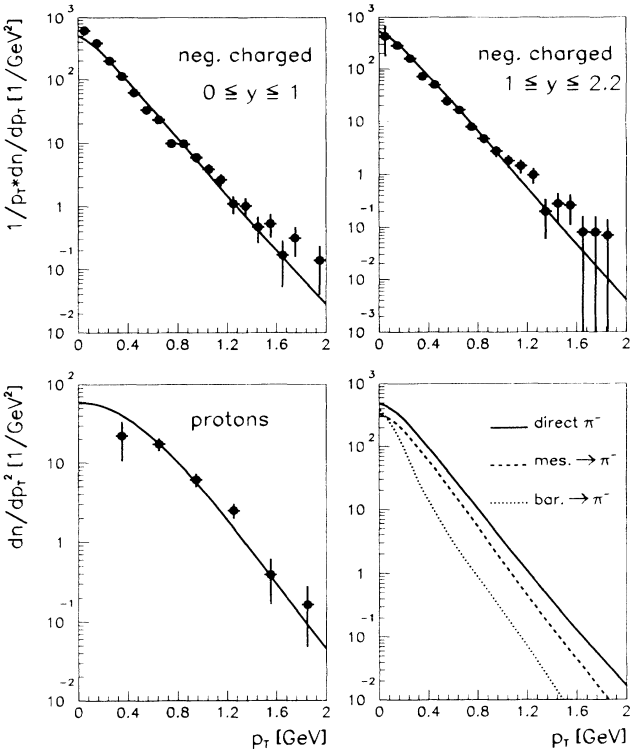

FIG. 4. Upper half: transverse momentum spectra of negatively charged secondaries of different rapidity intervals. Lower half: plots correspond to the entire accessible rapidity-interval ($-3 \le y \le +3$). In the lower left figure we plot the proton transverse-momentum distribution and in the lower right are the different contributions to the pion-$p_\perp$ distribution.

B. Rapidity distributions

Figure 5 shows the distributions in rapidity of negatively charged particles and protons. The latter were again exposed to the same corrections as for the $p_\perp$ distribution. Concerning the negatives it becomes very clear

[5]In our calculation these are ρ, ω, $K^*(892)$, Δ, and $\Sigma^*(1385)$.

that only about 40% of these are directly produced pions whereas the other are either kaons or pions from the decay of particle resonances. For the protons we have plotted additionally the different contributions to the spectrum. Contrary to the pions most of all protons are direct ones and only about one-fourth of them stems from the decay of baryon resonances. It can also be seen that the latter ones have a nearly constant y distribution and the maxima and minima of the net distribution are mainly caused by direct protons. That our model possibly underestimates the number of baryons at $y = \pm 2.5$ may be due to the fact that these baryons are not sufficiently thermalized.

In order to get an idea about the origin of the shape of the rapidity distributions Fig. 6 shows the longitudinal space-time evolution of the fireball-system. There one can find that the freeze-out process can be separated into two different space-time regions: First there is the so-called "simple-wave region" (SWR) which can be identified with the world-line of the forward-proceeding edge of the system. Second there is the so-called "nontrivial region" (NTR) which describes mainly the cooling from the interior. Contrary to the latter one the SWR consists of fluid cells of approximately the same (higher) rapidity. Thus one can interpret the peaks in the proton rapidity and the "shoulders" of the negative-particle rapidity at about ± 2 to be caused by particles emitted from the SWR and the more central rapidity region to be built up mainly by particles from the NTR. The comparatively higher probabilities of the SWR for protons than for pions can be directly related to the flow of baryonic charge depicted in the lower half of Fig. 6. There it is shown that the bulk of the baryonic charge is located near the edges of the system so that one can conclude that the SWR is baryon rich whereas the NTR is baryon poor.

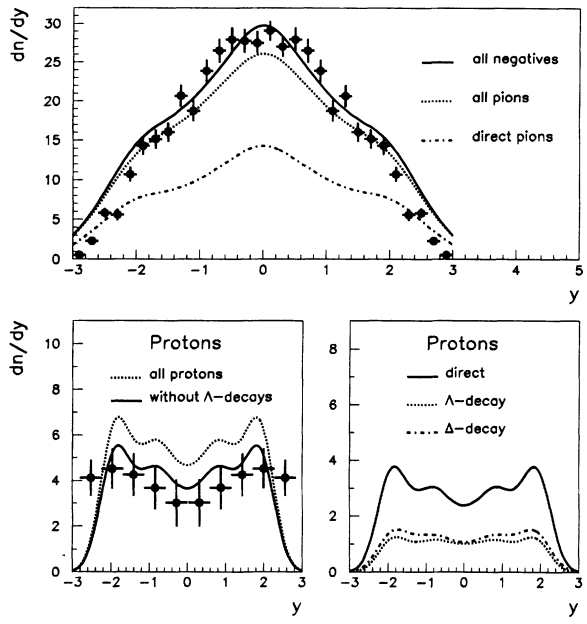

FIG. 5. Upper half: Rapidity distribution of negatively charged particles (solid line). Lower left: entire proton rapidity distribution [dashed, also plotted in Fig. 2(b)] and the resulting one after the subtraction of protons originating from the decay of Λ particles (solid, to be compared with the experimental data points). Lower right: main contributions to the proton-rapidity distribution; direct protons (solid), protons from Λ (dashed), and Δ decay (point-dashed). Like in experiment the upper $p_\perp$ cut was chosen equal to 2.0 GeV.

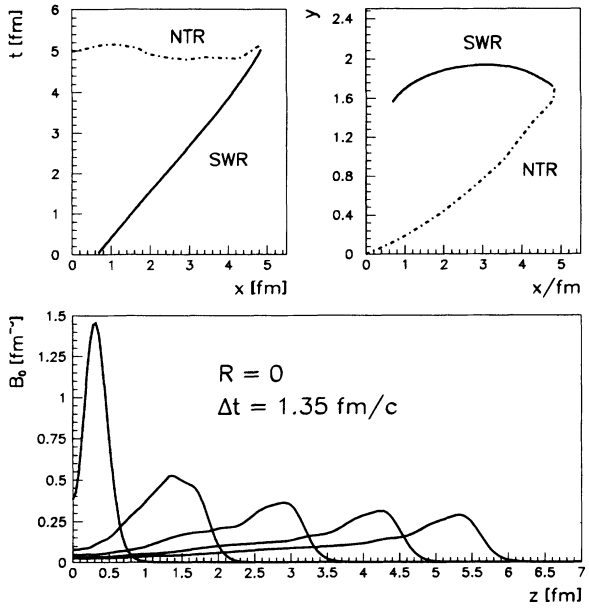

FIG. 6. Upper half: projection of the freeze-out hypersurface in the z-t plane at $R = 0$. For each of the two branches of this curve, simple wave region (SWR) and nontrivial region (NTR), we give in the upper right corner the fluid rapidity as a function of the longitudinal coordinate z. Lower half: baryon-density distributions B_0 of the fireball system in longitudinal direction at $R = 0$ in time steps of 1.35 fm/c (to illustrate the flow of baryonic charge).

C. Transvers radius

Naively one might expect the mean radial distance of pion production to be larger than the nuclear radius of sulphur because of radial expansion. Figure 7 however shows that the expansion time of the fireball is larger than its cooling time, so that the radial coordinate of freeze-out points cannot exceed the initial fireball radius which is 3.8 fm for $S+S$. This effect is a typical deflagration process and is discussed in more detail in Ref. [17]. It is thus not very surprising that the direct contribution to the transverse radius defined by Eq. (10) lies within the range of about 2.5 fm.

There exists a measurement of the transverse radius for

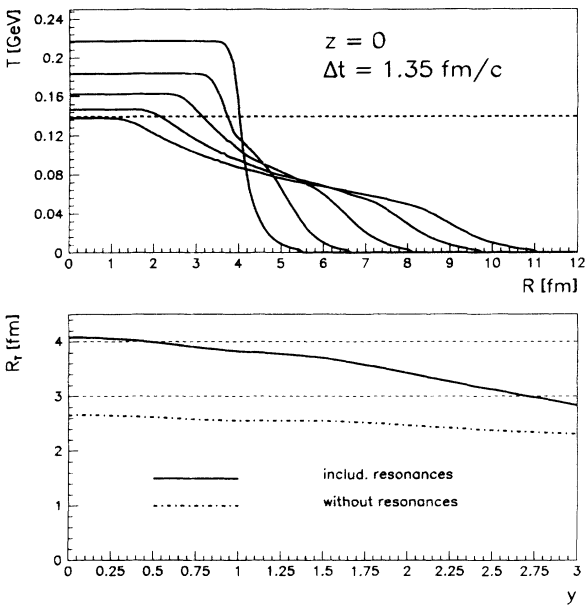

FIG. 7. Upper half: temperature distributions of the fireball system in radial direction at $z=0$ in time-steps of 1.35 fm/c. The decoupling-temperature of 0.139 GeV is plotted as a dashed horizontal line. Lower half: transverse radius $R_\perp$ with (solid) and without inclusion of resonance decay (point-dashed line). Here is also shown the region of $R_\perp$ consistent with the measurements of Ferenc [18] (3–4 fm, two dashed lines).

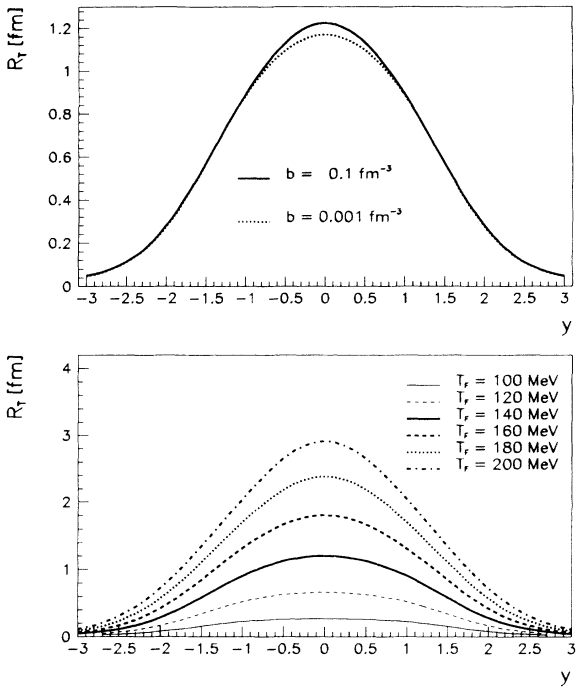

FIG. 8. Transverse radii of a pointlike source with the parameters chosen according to Table III. In the upper plot the temperature is kept constant at 139 MeV and in the lower plot the baryon density is kept constant at 5.58×10^{-3} fm^{-3}.

the "$S+S$-source" using Bose-Einstein correlations with the result [18]

$$R_\perp = 3.5 \pm 0.5 \text{fm} .$$

This value is consistent with our calculations. It is also remarkable that results including only direct pions yield much too low values for $R_\perp$. Thus it seems very important to consider resonance-decay in the calculation of transverse radii.

In order to get a deeper qualitative understanding of this decay contribution, we additionally investigated it for the case, where in Eqs. (11) and (12) the first terms are absent and thus all direct contributions vanish by definition. In particular, we varied first the baryon density b at fixed temperature T_F and then T_F at fixed b. The results are shown in Fig. 8, and the corresponding parameters are listed in Table III. It can be seen there that the baryon density has only a very small influence on the decay contribution to the transverse radius whereas this quantity is very sensitive to the freeze-out temperature. This means that if one is able to measure the y dependence of $R_\perp$ by pion interferometry more accurately, the variation of $R_\perp$ in the accessible rapidity range can also provide indirect information about the freeze-out temperature. In the case of the considered $S+S$ fireball, we observe that in our model the contribution from direct pions is nearly a constant over the entire rapidity interval and the variation of the net $R_\perp$ is caused by resonance-decay (cf. Fig. 7). Thus one could "measure" the freeze-out temperature by the variation of $R_\perp$.

The rapidity dependence of the resonance contribution to the transverse radius can be understood as follows: On

TABLE III. Parameters for pointlike sources in Fig. 8.

	b (10^{-3}/fm^3)	T_f (MeV)	μ_B (MeV)	μ_S (MeV)
T_f constant	1.00	139	14.0	1.37
	1000	139	436	83.8
b constant	5.58	100	366.8	25.1
	5.58	120	196.4	13.4
	5.58	140	71.0	7.35
	5.58	160	25.7	4.21
	5.58	180	11.1	2.55
	5.58	200	5.66	1.63

the average particles at large y have smaller $p_\perp$ (because of energy-momentum conservation). The mean rapidity of pions from resonance decay equals the mean rapidity of the resonance itself. Therefore the second term on the right-hand side of Eq. (12) is decreasing with increasing y, whereas the first term is almost independent of y as can be concluded from the radius for direct pions, where the second term is absent. A possible way to determine experimentally transverse radii with nearly negligible contributions from resonance decay would be not to consider pions but kaons, because in a thermal model the only significant decay contribution to kaon production comes from the $K^*(892)$ which itself is thermally suppressed relative to $K(494)$ by about a factor of 10. Thus Bose-Einstein-correlations with kaons would yield only the $R_\perp$-value from direct kaons, provided the statistics are sufficient.

D. Strangeness production

As was mentioned in the Introduction the problem of equilibration is not yet solved. It is expected that chemical equilibrium can be much easier achieved if the fireball spent some time of its evolution in the QGP phase, because there all quarks are massless and especially strange matter is assumed to be produced faster than in the hadronic-phase.[6] In the latter case it is even doubtful that the lifetime of the fireball suffices to reach chemical equilibrium, so that the investigation of strange-particle production may under certain circumstances serve as a signal for QGP formation. Our calculations are based on the existence of chemical equilibrium and the QGP-phase transition. These two assumptions could be tested by studying the spectra of strange particles.

In Fig. 9 we show the transverse-mass and rapidity spectra of Λ and K^0_S. There is a surprisingly good agreement of our calculations with experimental data obtained by the NA35 Collaboration [21]. In Table IV we give the total multiplicities of Λ, $\bar{\Lambda}$, and K^0_S. The values for Λ and K^0_S lie within the error-region of experiment whereas there is a discrepancy in the cas of the $\bar{\Lambda}$ yield, which—at the level of one standard deviation—is 4 times smaller in our model than in experiment.

There are several reasons which could account for this discrepancy: First it is conceivable that $\bar{\Lambda}$ particles freeze out at a higher temperature than the rest of the system. We checked this possibility and found that a temperature of about 160 MeV is sufficient to obtain the right multiplicity without disturbing very much the other "good" results. A higher decoupling temperature is associated with a smaller collision cross section inside the fireball [22]. It is however unclear why $\bar{\Lambda}$'s would react less with pions and nucleons than other particles.

Another reason is the fact that we are dealing with a very small absolute yield of $\bar{\Lambda}$ production. To consider the $\bar{\Lambda}$ discrepancy significant, one would have to require more stringent statistical criteria, i.e., standard deviations. Note also that the errors in the K^+ yield are of the order of 10%–20% (cf. Table IV) which amounts to 1–2 kaons.[7] However, because of strangeness conservation, a change of the kaon yield of this size must be compensated by an equal change in the number of other higher mass particles with strangeness. The resulting change in the $\bar{\Lambda}$ yield, the multiplicity of which is around 1, can then amount to several 100%. Finally, and most probably, we cannot expect chemical equilibrium to be established with less than say 10% accuracy. It is conceivable that $\bar{\Lambda}$ particles are more sensitive to the chemical equilibrium assumption and this could then serve as a test of this assumption.

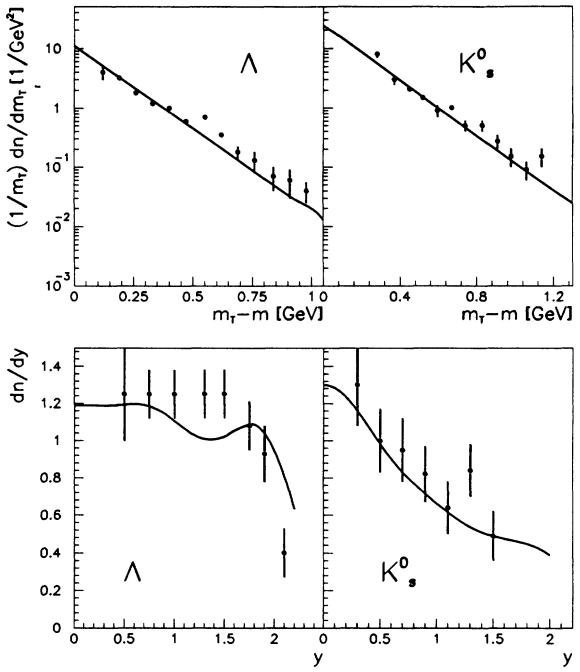

FIG. 9. Transverse-mass ($m_\perp$) and rapidity distributions of Λ and K^0_S in comparison with the experimental data from Ref. [21]. The rapidity intervals for the $m_\perp$ spectra are $1.0 \le y \le 2.2$ for Λ and $0.3 \le y \le 1.5$ for K^0_S. The transverse momentum ranges are $p_\perp \ge 0.5$ GeV for Λ and $p_\perp \ge 0.625$ GeV for K^0_S.

TABLE IV. Multiplicities of strange particles in comparison with experimental values from the NA35 experiment.

	Λ Mult.	$\bar{\Lambda}$ Mult.	K^0_S Mult.
Our values	8.77	0.38	12.53
NA35 exp.	8.2±0.9	1.5±0.4	10.7±2.0

[6]It was argued by Brown *et al.* [19] that a partical restoration of chiral symmetry with the increase of temperature in the hadronic phase might lead to a decrease of the strange particle masses and therefore could cause strangeness equilibration even in the hadronic phase. See however [20] where an opposite behavior of kaon masses with temperature is expected.

[7]A reduction of the number of K^+ by this amount has been suggested to occur due to the change of the dispersion relation for kaons in a nuclear medium [23].

V. CONCLUSIONS

In this study we introduced a new model for initial conditions of hydrodynamical expansion, which in particular takes into account baryons. Our treatment is based on the assumption of thermalized nucleons and from the comparison with data one can conclude from our results that this assumption appears to be valid for most of the baryonic matter. The nearly thermal $p_\perp$-distribution of the protons again underlines this property.

The observed rapidity and $p_\perp$ spectra of negatively charged particles and protons are well reproduced by the theory and a value for the transverse radius of the $S+S$ fireball is obtained purely from hydrodynamical considerations. Resonance decay appears to play an important role in transverse expansion. Furthermore, strangeness production was investigated and also compared to experiment. The agreement is again satisfactory.

Finally it has to be emphasized that the model can reproduce all these data provided one uses an equation of state obtained from lattice QCD which includes a phase transition from QGP to hadronic matter. It remains to be seen how the introduction of baryons in the EOS will modify this conclusion.

After the completion of this paper we received a preprint by Ishii and Muroya [11], in which part of the topics investigated by us are also studied. The authors use different hydrodynamical initial conditions, which they fix on a $\tau=\tau_0=1$ fm hypersurface according to Bjorken [8], and they introduce a phenomenological baryon-dependent EOS. However they do not consider resonance decay and do not study strangeness-production and sizes of the fireball.

ACKNOWLEDGMENTS

This work was supported in part by the Deutsche Forschungsgemeinschaft, Los Alamos National Laboratory, and the Deutsche Gesellschaft für Schwerionenforschung (GSI). We are indebted to D. Strottmann for instructive discussions. U.O. acknowledges the financial support of the DFG. J.B. would like to thank M. Plümer for countless useful discussions.

[1] L. D. Landau, Izv. Akad. Nauk SSSR **17**, 51 (1953).
[2] P. Carruthers and D. V. Minh, Phys. Rev. D **28**, 130 (1983).
[3] R. M. Weiner, in *Quark-Gluon-Plasma and the Landau Hydrodynamical Model,* Proceedings of Hadronic Matter under Extreme Conditions, Kiev, 1986, edited by G. M. Zinovjev and V. P. Shelest (unpublished), pp. 261–272.
[4] K. Wehrberger and R. M. Weiner, Phys. Rev. D **31**, 222 (1985).
[5] U. Ornik, F. W. Pottag, and R. M. Weiner, Phys. Rev. Lett. **63**, 2641 (1989).
[6] U. Ornik and R. M. Weiner, Phys. Lett. B **263**, 503 (1991).
[7] U. Ornik and R. M. Weiner, Los Alamos Report No. LA-UR 92-906 (unpublished).
[8] J. D. Bjorken, Phys. Rev. D **27**, 140 (1983).
[9] S. Wenig, Ph.D. thesis, GSI Report No. 90-23, 1990 (unpublished).
[10] S. Z. Belenkij and G.A. Milekhin, Zh. Eksp. Teor. Fiz. **29**, 20 (1955) [Sov. Phys. JETP **2**, 14 (1956)].
[11] T. Ishii and S. Muroya, Waseda University Report No. 92-6 (unpublished).
[12] F. Cooper, G. Frye, and E. Schonberg, Phys. Rev. D **11**, 192 (1975).
[13] J. Sollfrank, P. Koch, and U. Heinz, Z. Phys. C **52**, 593 (1991).
[14] H. Pilkuhn, *The Interaction of Hadrons* (North-Holland, Amsterdam, 1967).
[15] J. Bolz, U. Ornik, and R. M. Weiner, GSI Scientific Report No. 92-1, 1992 (unpublished), p. 156.
[16] U. Ornik, in *Hydrodynamics from SPS to SSC,* Proceedings of the International Meeting on Relativistic Aspects in Nuclear Physics, Rio de Janeiro, Brazil, 1991, edited by T. Kodama (unpublished).
[17] B. R. Schlei, U. Ornik, M. Plümer, and R. M. Weiner, Los Alamos Report No. LA-UR-92-1058 (unpublished).
[18] D. Ferenc, Proceedings of Quark Matter 91 (unpublished).
[19] G. E. Brown *et al.*, Phys. Rev. C **43**, 1881 (1991).
[20] J. P. Blaizot and R. Mendez Galain, Phys. Lett. B **271**, 32 (1991).
[21] NA35 Collaboration, J. Bartke *et al.*, Z. Phys. C **48**, 191 (1990).
[22] U. Heinz, K. S. Lee, and E. Schnedermann, Z. Phys. C **48**, 525 (1990).
[23] C. Gong, J. Phys. G **18**, L123 (1992).

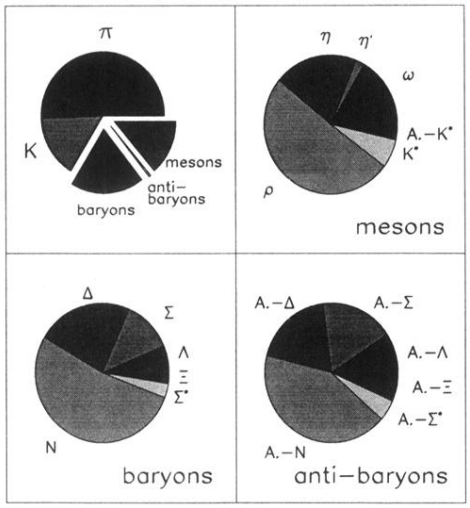

FIG. 3. Chemical composition of frozen-out particles. In the upper left quarter we give a general composition. The subcompositions of the three offset sectors "mesons," "baryons," and "antibaryons" are shown in the remaining parts.